Molecular Properties of ClpAP Protease of *Escherichia coli*: ATP-Dependent Association of ClpA and ClpP

Michael R. Maurizi,*,‡ Satyendra K. Singh,‡,§ Mark W. Thompson,‡,|| Martin Kessel,‡,|| and Ann Ginsburg⊥

Laboratory of Cell Biology, National Cancer Institute, and Section on Protein Chemistry, Laboratory of Biochemistry, National Heart, Lung, and Blood Institute, National Institutes of Health, Bethesda, Maryland 20892

Received December 16, 1997; Revised Manuscript Received March 18, 1998

ABSTRACT: The ClpAP protease from *Escherichia coli* consists of the ATP-binding regulatory component, ClpA (subunit M_r 84 165), and the proteolytic component, ClpP (subunit M_r 21 563). Our hydrodynamic studies demonstrate that the predominant forms of these proteins in solution correspond to those observed by electron microscopy. ClpP and proClpP(SA), which in electron micrographs appear to have subunits arranged in rings of seven subunits, were found by ultracentrifugation to have $s_{20,w}$ values of 12.2 and 13.2 S and molecular weights of 300 000 and 324 000 ± 3000, respectively, indicating that the native form of each consists of two such rings. The two intact rings of ClpP were separated in the presence of ≥0.1 M sulfate at low temperatures, suggesting that ring−ring contacts are polar in nature and more easily disrupted than subunit contacts within individual rings. Sedimentation equilibrium analysis indicated that ClpA purified without nucleotide exists as an equilibrium mixture of monomers and dimers with $K_a = (1.0 \pm 0.2) \times 10^5$ M^{-1} and that, upon addition of MgATP or adenosine 5′-*O*-(3-thiotriphosphate), ClpA subunits associated to a form with M_r 505 000 ± 5000, consistent with the hexameric structure seen by electron microscopy. Sedimentation velocity and gel-filtration analysis showed that the nucleotide-promoted hexamer of ClpA ($s_{20,w}$ = 17.2 S) binds tightly to ClpP producing species with $s_{20,w}$ values of 21 and 27 S (f/f_0 = 1.5 and 1.8, respectively), consistent with electron micrographs of ClpAP that show a single tetradecamer of ClpP associated with either one or two ClpA hexamers [Kessel et al. (1995) *J. Mol. Biol. 250*, 587−594]. Under assay conditions in the presence of ATP and Mg^{2+}, the apparent dissociation constant of hexameric ClpA and tetradecameric ClpP was ∼4 ± 2 nM. By the method of continuous variation, the optimal ratio of ClpA to ClpP in the active complex was 2:1. The specific activities of limiting ClpA and ClpP determined in the presence of an excess of the other component indicated that the second molecule of ClpA provides very little additional activation of ClpP.

ATP-dependent proteases play a major role in rapid intracellular proteolysis in both prokaryotes and eukaryotes. *Escherichia coli* has several soluble ATP-dependent proteases, Lon, ClpAP, ClpXP, and ClpYQ (HslUV) (*1*−*6*) and a membrane-associated protease, FtsH, which is an integral membrane protein with large cytoplasmic domains with ATP-dependent proteolytic activity (*7*). In vivo, the proteases are highly selective in their targets; for example, Lon is required for degradation of *E. coli* SulA (*8*), RcsA (*9*), and phage λ N protein (*10*); ClpAP degrades *E. coli* MazE (*11*) and several β-galactosidase fusion proteins (*12*); ClpXP has very different targets, degrading the highly unstable λ O protein (*4*, *13*) and other proteins (*14*−*16*); and FtsH targets the heat shock regulatory factor, σ^{32} (*7*, *17*). In addition to promoting proteolysis, these proteases catalyze ATP-dependent protein folding and unfolding [referred to as protein remodeling (*18*)] and thus function as molecular chaperones both in vivo and in vitro (*18*, *19*).

The ATPase and proteolytic activities of ATP-dependent proteases reside in different subunits or in separate domains of a single polypeptide chain. *E. coli* ClpAP and ClpXP serve as good models of the former type. ClpAP is a complex of two heterologous proteins, ClpA, which has two ATP binding sites and catalyzes the ATPase activity, and ClpP, which contains the proteolytic active site (*12*, *20*−*22*). ClpXP is a complex of ClpP and a distinct, though related, single-domain ATPase, ClpX (*23*). Electron micrographs indicate that ClpAP (*24*) and ClpXP (*23*) are similar in architecture to the eukaryotic 26S proteasome (*25*, *26*), a stacked-ring complex with an inner core of proteolytic subunits flanked by the ATPase or other regulatory complexes. The structures appear to be designed to allow protein substrates only limited access to the proteolytic active sites and to require that they interact first with the ATPase domains. The ATPase/chaperone component can unfold or structurally remodel the protein to enable it either to enter the proteolytic active sites or to be released and allowed to refold (*27*).

Although the complexes formed by the components of ATP-dependent proteases have been described, little is

* To whom correspondence should be addressed at Laboratory of Cell Biology, National Cancer Institute, Bldg. 37, Room 1B09, Bethesda, MD 20892. Phone 301-496-7961; FAX 301-402-0450.

‡ Laboratory of Cell Biology, National Cancer Institute.

§ Present address: Department of Neurosurgery, University of Maryland Medical School, 685 W Baltimore St., MSTF Rm 623, Baltimore, MD 21201.

|| Present address: Laboratory of Structural Biology Research, NIAMS, Bldg. 6, Room B2-34, Bethesda, MD 20892.

⊥ Section on Protein Chemistry, Laboratory of Biochemistry, National Heart, Lung, and Blood Institute.

S0006-2960(97)03093-6
Published on Web 05/07/1998

known about the solution properties of these enzymes or about changes in subunit interactions during catalysis. In this paper, we report hydrodynamic properties of the oligomeric forms of ClpA and ClpP and confirm that, in the presence of ATP analogues, ClpA subunits form a hexamer that interacts with ClpP. A stable, stoichiometric complex of ClpA hexamers and ClpP tetradecamers is formed in solution and is required for ATP-dependent protein and oligopeptide degradation. Preliminary reports of portions of these studies have appeared (*28*, *29*).

EXPERIMENTAL PROCEDURES

Enzyme Preparation and Assay. ClpA and ClpP were purified as described elsewhere (*30*) from extracts of cells with multicopy plasmids carrying the respective genes (*30*−*32*). Mutant ClpP proteins were purified by the same procedure used for wild-type ClpP. Enzymes were prepared and stored in buffer B [50 mM Tris-HCl, pH 7.5 at 25 °C, 1 mM EDTA, and 10% (v/v) glycerol] to which was added 0.3 M KCl and 1 mM dithiothreitol (DTT).[1] Protein degradation was measured as the acid solubilization of [^{3}H]-α-casein in a reaction mixture containing 50 mM Tris-HCl (pH 8.0 at 25 °C), 25 mM $MgCl_2$, 0.1 M KCl, 4 mM ATP, and 30−50 μg/mL α-casein; ATPase activity was measured by the release of phosphate from [^{32}P]ATP as described elsewhere (*30*).

Analytical Ultracentrifugation. Prior to ultracentrifugation experiments, proteins were either dialyzed against two changes of buffer B or passed through a Sepharose 6 column equilibrated with buffer B. KCl (0.10−0.30 M), ATPγS (1−2 mM), DTT (1 mM), and $MgCl_2$ (20−25 mM) were present as indicated. Beckman model E calibrations, schlieren photographs, and viscosity measurements were as described previously (*34*). Schlieren plates were read and analyzed as in Shrake et al. (*35*). Solvent densities were measured by pycnometry at 25 or 20 °C with a model DMA-58 density meter (Anton Paar). The following are the measured densities relative to that of water at the same temperature (ρ/ρ_0) and the relative viscosities (η/η_0) measured at 25 °C: for buffer B with 0.2 M KCl, $\rho/\rho_0 = 1.038$ and $\eta/\eta_0 = 1.415$; for buffer B with 0.30 M KCl, $\rho/\rho_0 = 1.047$ and $\eta/\eta_0 = 1.418$; for buffer B without glycerol with 0.10 M KCl, $\rho/\rho_0 = 1.0074$ and $\eta/\eta_0 = 1.017$; for buffer B without glycerol with 0.3 M KCl, $\rho/\rho_0 = 1.0084$ and $\eta/\eta_0 = 1.020$. Protein partial specific volumes were calculated from amino acid compositions (*36*) obtained from DNA sequence data (*22*, *33*). Calculated values of partial specific volumes ($\bar{v}$) are 0.723, 0.723, and 0.725 mL/g for ClpA, proClpP(SA), and mature ClpP, respectively.

Sedimentation velocity experiments were conducted at 20 °C with a Beckman model E ultracentrifuge equipped with schlieren optics (with phase plate) and a two-place AnD aluminum rotor and in a Beckman optima model XL-A (absorption optics) equipped with a four-place An-Ti (titanium) rotor. Analytical cells had 12 mm, 4°, Kel F-coated double sector centerpieces and sapphire plane windows (model E) or plane, far-UV quartz windows (model XL-A). Loading volumes were 0.34 mL of protein solution and 0.35 mL of the appropriate buffer. In the model E, the drive was started immediately and the rotor was allowed to coast at 3000−5000 rpm until the vacuum was <0.5 μm and the rotor temperature registered 20.0 °C. After the rotor was accelerated to the desired speed, photographs were taken at 4 min intervals for 40−60 min. Data were analyzed by measuring the maximum ordinate of the schlieren pattern as a function of the distance from the center of rotation (using the air reference holes of the counterbalance) and time. In the model XL-A, the rotor was immediately accelerated to 3000 rpm and maintained at this speed until the temperature was 20.0 °C and the vacuum was <1 μm (30−60 min). Then, ≥15 radial scans at 4 min intervals were programmed in the continuous mode with 0.003 cm increments (1−3 averages) to begin when the rotor reached the preset high speed. Data were collected and boundary movements were monitored by A. P. Minton's TRACKER program,[2] which was run with DESQ view 386 quarterdeck installed on a 386 computer interfaced to the model XL-A. Sedimentation velocity files from the model XL-A were analyzed with Beckman programs operating under MS DOS or Windows: XLAVEL for determining inflection points of boundaries from dA/dr versus r plots for calculating sedimentation coefficients (comparable to results obtained from schlieren patterns), VELGAMMA for diffusion coefficients (D) by second moment/boundary spreading analyses (s/D coefficients), and time derivative (dc/dt) analysis (s/D coefficients). Diffusion coefficients were also obtained by low-speed boundary spreading at 10 000 rpm with a capillary synthetic boundary cell to layer buffer onto the protein solution at low speed; data were analyzed as described (*37*). Molecular weight was calculated from the Svedberg equation [$M_r = RTs/D(1 - \bar{v}\rho)$], where $\bar{v}$ is the partial specific volume of the protein, R is the gas constant, and T is the absolute temperature).

Sedimentation equilibrium experiments were conducted in the Beckman model XL-A at 4.0 °C. Protein solution column heights were 0.080−0.190 mL and the sample buffer in the left sector was 0.010 mL higher. Radial and wavelength scans were made at 3000 rpm before the rotor was accelerated to the desired speed. Autoscans were collected at 6 h intervals to follow the progress in reaching equilibrium (wavelengths were not changed until data collection was complete). After equilibrium was reached, radial scans were made in the step mode at 0.001 cm increments with 9−19 averages. Baselines were measured at the same speeds under the same scan conditions after overspeeding to 56 000 rpm for 4−5 h to sediment proteins. Most baselines were smooth and were constrained to averaged values (<0.05) in the various sedimentation equilibrium analysis programs of A. P. Minton. When small distortions were present in measured baselines (possibly due to oil contamination on the cell windows), baseline files were subtracted point by point from sedimentation equilibrium data files by using the DIFSCAN program of A. P. Minton before analysis. This procedure improved statistical calculations but did not change the shape of the gradients. Data from

[1] Abbreviations: DTT, dithiothreitol; proClpP(SA), unprocessed ClpP that has a serine to alanine mutation at the active site and retains the amino-terminal 14 amino acid propeptide (*33*); ATPγS, adenosine 5′-(3-thiotriphosphate).

[2] Programs of Allen P. Minton, NIDDK, NIH, Bethesda, MD 20892, for analysis of sedimentation equilibrium data obtained from the Beckman model XL-A can be downloaded from the following World Wide Web site: http://bbri-www.eri.harvard.edu/RASMB/rasmb.html.

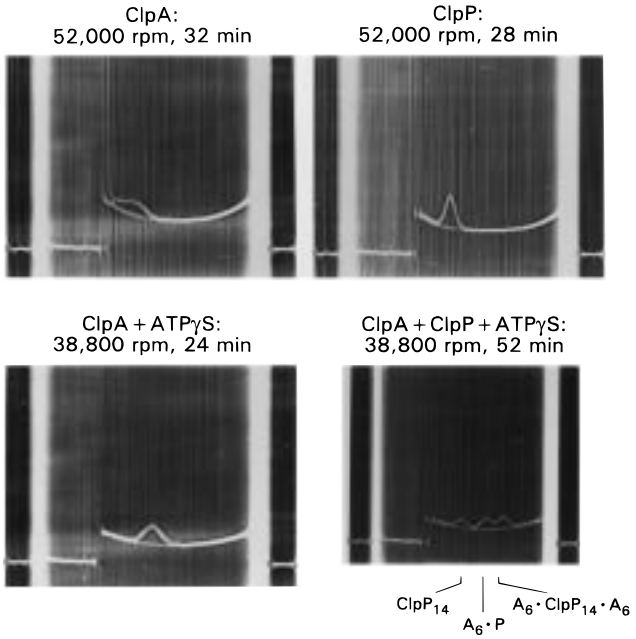

FIGURE 1: Sedimentation velocity ultracentrifugation of ClpA, ClpP, and ClpAP complexes. Velocity sedimentation was performed in a Beckman Model E analytical ultracentrifuge with schlieren optics, as described under Experimental Procedures. The buffer in all cases was buffer B plus 0.3 M KCl and 1 mM DTT and the temperature was 20 °C. Where indicated, 25 mM $MgCl_2$ and 1 mM ATPγS were added to the buffer. The proteins (2−4 mg/mL ClpA and/or 2−6 mg/mL ClpP) had been gel-filtered through a Sepharose 6 column equilibrated with buffer B plus 0.3 M KCl and 1 mM DTT. Representative photographs of schlieren patterns (including counterbalance air reference holes) are shown with the time after reaching the indicated speed. The direction of sedimentation is to the right; buffer and protein menisci are to the left; and the sedimenting boundary is shown by the concentration gradient with respect to radial position (dn/dr) relative to that of the reference buffer. The samples and times at which the schlieren patterns were recorded are shown above the panels.

the model XL-A were analyzed with programs written by A. P. Minton for analysis of sedimentation equilibrium in solutions of a single macrosolute in the context of models for equilibrium self-association. Weighted fits to take into account the noise characteristics of the instrument, global fits of up to three data sets, and equilibria models for nonassociating as well as associating macromolecules were used.[2]

Other Analytical Methods. Gel filtration was conducted at 5 °C using Pharmacia Superose 6 or Superdex 200 columns (1 × 30 cm). The buffer was buffer B containing 0.2 M KCl and 2 mM DTT, with or without 25 mM $MgCl_2$ and 2 mM ATP, 2 mM ADP, or 1 mM ATPγS. The flow rate was 0.2−0.3 mL/min. Protein was monitored by absorbance at 280 nm. Electron microscopy of ClpP negatively stained with uranyl acetate was performed as described elsewhere (*24*).

RESULTS

Analytical Ultracentrifugation of ClpA. Figure 1 shows photographs of schlieren patterns taken at 24−32 min after reaching speed for ClpA ± 1 mM ATPγS and $MgCl_2$. The broadness of the sedimenting boundary of ClpA in the absence of nucleotide is due to the existence of a monomer−dimer equilibrium as shown below. ClpA in the presence of the nucleotide was homogeneous with respect to sedimentation rate. The large increase in the sedimentation coefficient (from ∼9 to 17 S; Table 1) and the shift in elution position of ClpA seen by gel filtration indicate that binding of ATP or nonhydrolyzable analogues promotes association of ClpA subunits.

Table 1: Summary of Analytical Ultracentrifugation Results on Single Components[a]

protein sample	$s_{20,w}$[b] (±0.1) (S)	$D_{20,w}$ (±0.2 × 10^7) (cm^2/s)	M_r[c] (±5%)	M_r[d] (±5%)
ClpA	8.7 (5.4; 9.5)[e]			(2A ⇄ A_2)[f]
ClpA + ATPγS	17.2			505 000
ClpP	12.2	3.65[g]	300 000	(unstable)
	12.2[h]	3.6[h]	300 000	
ClpP/5 °C; sulfate[i]	7.9[j]			
ClpP/20 °C; sulfate[k]	12.2			
ProClpP(SA)	13.2	3.7[g]	312 000	324 300

[a] Using buffer B ± 10% (v/v) glycerol, pH 7.5, for equilibration of samples. [b] Measured from inflection points and second moment analysis of absorbance boundaries or peaks in schlieren patterns as functions of radial position and time, unless otherwise indicated. [c] From s/D and the Svedberg equation. [d] From sedimentation equilibrium. [e] From time derivative analysis of model XL-A files for $g(s^*)$: two-Gaussian fit (*44*). [f] $K_A' = (1.0 \pm 0.2) \times 10^5$ $(M_{monomer})^{-1}$ for monomer/dimer equilibrium. [g] From low-speed (10 000 rpm) and high-speed (40 000 rpm) boundary spreading analysis in the absence of glycerol (*37*). [h] Using the time-derivative analysis of Stafford (*45*) and two ClpP gradients obtained after 56 and 60 min at 40 000 rpm, 20.0 °C, in buffer without glycerol. [i] After gel filtration through Sepharose 6 column at 4 °C in the presence of 0.1 M sodium sulfate in 0.02 M sodium phosphate buffer at pH 7.0, the ClpP was kept on ice and centrifuged at 5 °C and 52 000 rpm. A single Gaussian gave a good fit of the $g(s^*)$ junction, centered at 5.0 S, in the time-derivative analysis of Stafford (*45*). [j] Predicted $s_{20,w}$ for one-half ClpP is $12.2/(2)^{2/3} \approx 7.7$ S. [k] The rotor and sample used for analysis of ClpP in the presence of sulfate at 5 °C were warmed to 20 °C, and centrifugation was repeated.

Sedimentation equilibrium studies of ClpA in the absence of nucleotide at pH 7.5 are shown in Figure 2A. The data obtained with ClpA in the absence of nucleotide with these and other data files best fit a model for a monomer−dimer equilibrium of ClpA with an association constant of (1.0 ± 0.2) × 10^5 M^{-1} and monomer M_r 84 000. The upper panel in Figure 2A shows the residuals from the χ^2 error analysis, where $\chi^2 = \sum[(y_i - y_{cal}c_i)/s_i]^2$ for the weighted fitting.[2] The residuals in Figure 2 show a random distribution of ∼±0.01 absorbance, which is the same as the root-mean-square error. The data could not be fitted to models involving no dimerization or assumptions of monomer equilibria with oligomeric states greater than that of the dimer with reasonable error estimates. These observations are in agreement with the sedimentation velocity results illustrated in Figure 1 in which only a single, slowly sedimenting, broad boundary is observed for ClpA in the absence of nucleotide.

Sedimentation equilibrium data for ClpA in the presence of a saturating concentration of the nonhydrolyzable analogue ATPγS and 25 mM $MgCl_2$ at pH 7.5 are shown in Figure 2B. Data files collected at 298 nm (at which wavelength the nucleotide analogue does not absorb light) after 70 h at 4000 rpm and 47 h at 3700 rpm were subjected to a global, weighted, nonlinear least-squares analysis. The data were fit to a model of a single species having the molecular weight of a hexamer of ClpA (505 000 M_r; solid line of Figure 2B). The residuals from the χ^2 error analysis are shown in the upper panel. The data did not fit a model for a dimer−

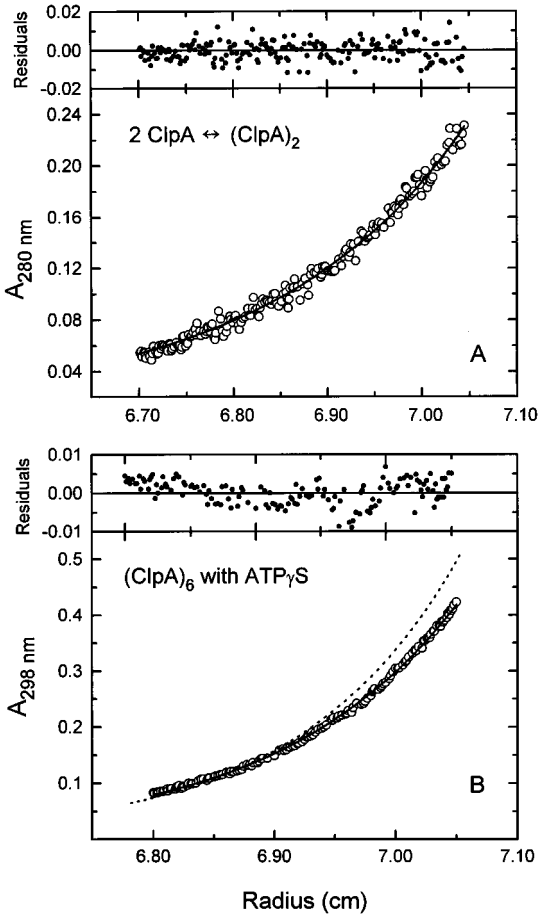

FIGURE 2: Sedimentation equilibrium ultracentrifugation of ClpA. (A) Sedimentation of ClpA in the absence of nucleotide. Conditions of the model XL-A run were 0.190 mL of ClpA (0.5 and 0.2 mg/mL) in buffer B plus 0.3 M KCl and 1 mM DTT at 4 °C. A weighted simultaneous fit of data from scans at 280 nm (after baseline subtraction) obtained for 0.5 mg/mL of ClpA after 53 h at 7000 rpm (○), 0.2 mg/mL of ClpA after 53 h at 7000 rpm, and 0.5 mg/mL of ClpA after 74 h at 7000 rpm to a model for a monomer/dimer equilibrium with $K_A' = 1.0 \times 10^5$ $(M_{monomer})^{-1}$ is shown by the solid line. The upper panel shows a plot of the residuals from the global fitting procedure for the data in the figure; the overall RMS error is 0.012. (B) ClpA in the presence of ATPγS and $MgCl_2$ at 4.0 °C. Conditions were the same as in panel A except that column heights were 0.150 mL of ClpA at 2.5 mg/mL concentration in buffer B with 1 mM ATPγS and 25 mM $MgCl_2$ present. After overspeeding, the data (○) shown are from a scan at 298 nm made after 70 h at 4000 rpm. A weighted simultaneous fit of this scan and another made after 47 h at 3700 rpm to a model for a noninteracting, single species of 505 000 M_r give the solid line with an overall RMS error of 0.0075. A plot of the residuals for the illustrated data is shown in the upper panel. A simulated gradient for a 7-mer of ClpA at the same rotor speed of 4000 rpm, 0.150 mL column height, temperature, and buoyancy ($1 - \bar{v}\rho$) is shown by the dotted line.

hexamer equilibrium without a 3-fold increase in the error of the fit and a value for $K_{1,3}$ consistent with complete association to a hexamer at the concentration of ClpA present. The dotted line in Figure 2B shows a simulated gradient expected for a heptamer (M_r 556 000) under the same conditions. It is apparent that a heptamer of ClpA would form a much steeper gradient than observed.

ATP or ATPγS Is Required To Maintain the Hexameric Form of ClpA. Self-association of ClpA is also evident from the shift in elution position of ClpA upon gel filtration in the presence of ATP or ATPγS (*31*). Association of ClpA

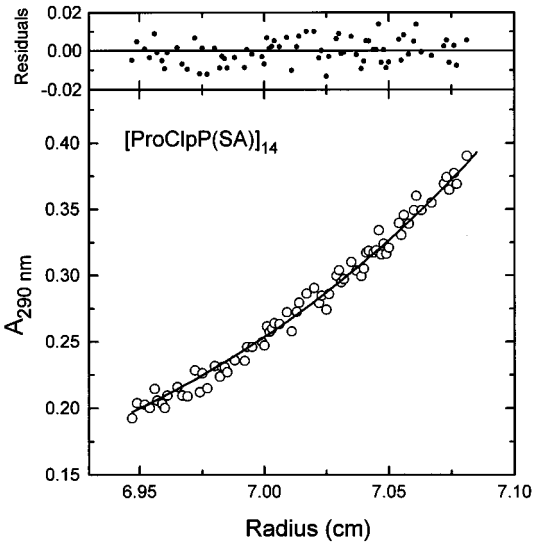

FIGURE 3: Sedimentation equilibrium ultracentrifugation of proClpP(SA). Conditions of the run in the model XL-A were 0.080 mL of 2.9 mg/mL ProClpP(SA) in buffer B plus 0.1 M KCl and 1 mM DTT at 4 °C. The data (○) shown are from a radial scan taken at 290 nm after 48 h at 4700 rpm. The solid line shows a simultaneous weighted fit of the data illustrated together with comparable data obtained after 54 h at 4700 rpm and 48 h at 4800 rpm to a model for an ideal, monodisperse (noninteracting) macromolecule of 324 400 M_r. The overall RMS error is 0.007. A plot of the residuals from the fitting procedure to the illustrated data is shown in the upper panel.

requires the continuous presence of ATP or ATPγS. ClpA hexamers assembled by pretreatment with ATPγS dissociated to predominantly dimeric form when the ClpA was run over the column in the absence of nucleotide, although about 20% of the ClpA hexamer remained even after the 6−10 min required to run the gel-filtration column (data not shown). Enzymatic activity and light scattering measurements indicate that ClpA assembles in the time of mixing (≤30 s) and dissociates very slowly in the presence of nucleotide (S. K. Singh and M. R. Maurizi, unpublished data).

Sedimentation Analysis of ClpP. Image reconstructions of electron micrographs of mature ClpP and the mutant proClpP(SA) particles show 7-fold symmetry (*24*). Combined with gel filtration and sedimentation equilibrium data, which gave molecular weights of 230−270 000, the native ClpP structure was proposed to be contain 14 subunits (M_r 300 000). Scanning transmission electron microscopy (*38*) gave an average mass of 300 000, and recent X-ray crystal structure analysis of ClpP confirmed the tetradecameric structure (*39*).

The consistently lower molecular weight of ClpP obtained by sedimentation equilibrium probably reflected the failure to reach true equilibrium because of ClpP instability over extended periods. A ClpP mutant, proClpP(SA), proved to be better behaved, and the results from a sedimentation equilibrium experiment are shown in Figure 3. The data fit a model for a single tetradecameric species of proClpP(SA) with a M_r of 324 400. The residuals (upper panel, Figure 3) showed an RMS error of <0.010. These results suggested that the presence of the propeptide in proClpP(SA), which may occupy the central aqueous cavity in the tetradecamer (*24*), may contribute to the stability of ring−ring interactions.

Native ClpP was stable during high-speed sedimentation for 2 h at 20 °C in the presence or absence of glycerol (e.g.,

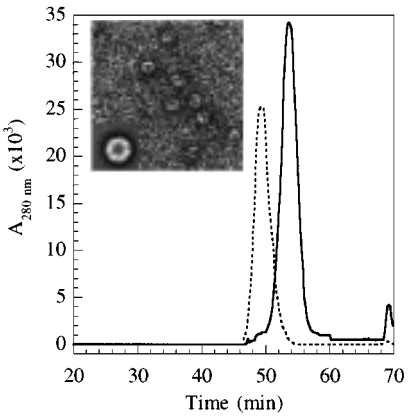

FIGURE 4: Isolation of half-ClpP by gel filtration. ClpP (100 μL of 3.5 mg/mL in buffer B plus 0.3 M KCl and 1 mM DTT) was run over a Superdex 200 column (1 × 30 cm) at 4 °C in either 50 mM Tris-HCl, pH 7.5, with 0.2 M KCl (dotted line) or 20 mM sodium phosphate, pH 7.2, with 0.1 M sodium sulfate (solid line). (Inset) Portion of an electron micrograph of negatively stained half-ClpP, with an inset showing an averaged image (~11 nm diameter) obtained from 200 particles.

Figures 1 and 5B). Data obtained in several independent experiments gave an average sedimentation coefficient of 12.2 S. A translational diffusion coefficient ($D_{20,w}$) of (3.6 ± 0.2) × 10^{-7} cm^2/s was obtained from sedimentation data and from low-speed boundary spreading analysis. The molecular weight for ClpP calculated from these data by use of the Svedberg equation was 300 000 (Table 1). Similar analyses of proClpP(SA) ($s_{20,w}$ = 13.2 S and $D_{20,w}$ = 3.7 × 10^{-7} cm^2/s) gave a calculated molecular weight of 312 000 (Table 1).

Dissociation of ClpP into Single Rings. The aberrant mobility of ClpP on silica columns and on Superose 6 columns may have been caused by two factors: interaction of ClpP with those matrixes and partial separation of the two ClpP rings. When run over gel-filtration columns in the presence of high concentrations (≥0.1 M) of sulfate at ≤4 °C, ClpP migrated as expected for a protein half the size of native tetradecamer, whereas under identical conditions but at room temperature, ClpP migrated as expected for the tetradecamer (Figure 4). Sedimentation velocity analysis of ClpP at 4 °C in the presence of sulfate revealed a species with $s_{20,w}$ = 7.9 (Figure 5A and Table 1), very close to the value of 7.7 predicted for a molecule half the size of native ClpP. Electron micrographs of the apparent half-ClpP molecules showed rings that were very similar to those of native ClpP, although the images appeared to have lower intensity (inset, Figure 4). Symmetry analysis and averaging of the half-ClpP images indicated a clear 7-fold symmetry. Thus, the combination of low temperature and high concentrations of anions causes the rings of ClpP to separate without disrupting the intersubunit contacts within the rings.

Half-ClpP molecules were stable for 1−2 days at 0−4 °C and migrated identically when reapplied to the gel-filtration column under the same conditions. However, if the separated rings are allowed to warm to 20 °C, the $s_{20,w}$ measured by sedimentation velocity analysis was 12.2 S, corresponding to the native tetradecamer (Figure 5B and Table 1). Thus, separated ClpP rings remain competent to reassociate to form the native tetradecamer. ClpP treated with sulfate at 4 °C also retained the ability to express peptidase activity against

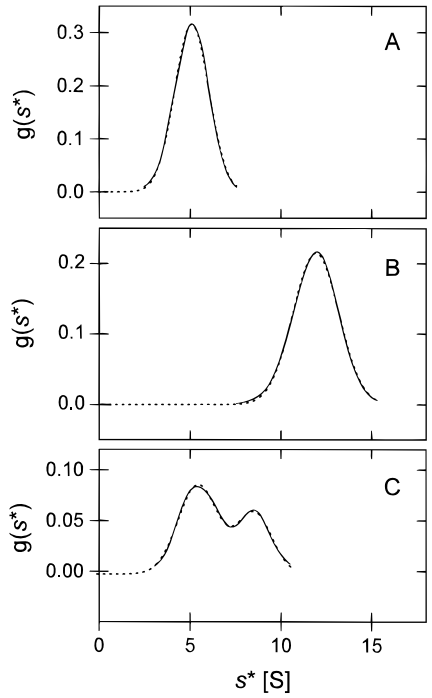

FIGURE 5: Sedimentation of ClpP in the presence of sulfate. ClpP (≈3.5 mg/mL) was run over a Superose 200 column in 0.1 M sodium sulfate in 20 mM sodium phosphate buffer, pH 7.2, at 4 °C. The ClpP, which migrated in the position expected for molecules with half the native size, was subjected to sedimentation velocity analysis in the XL-A centrifuge at 52 000 rpm. (A) Sedimentation was at 5 °C and care was taken to keep the ClpP (1.5 mg/mL) ≤5 °C at all times. (B) ClpP (1.3 mg/mL) was warmed to 20 °C before ultracentrifugation at 20 °C. (C) The sample from panel B was rerun within 1 h after the cell and rotor were cooled to 5 °C. Results illustrated in each panel are from two late concentration profiles (3 averages/scan) having harmonic sedimentation times of 60 (panel B) and 38 min (panels A and C). The solid lines show the apparent distribution functions $g(s^*)$ vs sedimentation coefficient in Svedberg units (*44*). The dotted lines show single Gaussian fits in panels A and B and a two-Gaussian fit in panel C. Observed sedimentation coefficients of solutes are given by s^* values at the maxima.

succinyl-Leu-Tyr-(aminomethyl)coumarin when assayed at 37 °C in the normal assay buffer or in the presence of sulfate (data not shown), although we cannot rule out that the separated rings, despite the high dilution (<10 μg/mL), reassociated under assay conditions.

Although ClpP stored in buffer with KCl dissociated rapidly after treatment with 0.1 M sulfate at 4 °C (Figure 4), dissociation was somewhat slower for ClpP that had been exposed to sulfate at 20 °C and then cooled. Figure 5C shows that, when ClpP in sulfate at 20 °C was cooled to 4 °C for less than 1 h, two separate species could be detected by sedimentation velocity analysis. About 75% of the mixture gave a calculated $s_{20,w}$ close to that expected for heptameric ClpP and the remainder corresponded to the tetradecamer. (Note that no temperature correction was applied for the sedimentation coefficients listed on the axes in Figure 5.)

Analysis of the Complexes between ClpA and ClpP. ClpA and ClpP do not interact tightly in the absence of ATP and Mg (*20*, *21*, *30*). Sedimentation velocity experiments using schlieren optics was used to show the formation of complexes between ClpA and ClpP in the presence of ATPγS and Mg (Figure 1). In the absence of ATPγS, ClpA and ClpP sep-

Table 2: Sedimentation Velocity Results with Mixtures of ClpA and ClpP[a]

mixture	$s_{20,w}$[a] (S)	probable species	f/f_0[b]
excess $(ClpA)_6$	17	$(ClpA)_6$	1.4
	27[c]	$(ClpA)_6$·$(ClpP)_{14}$·$(ClpA)_6$	1.8
excess $(ClpP)_{14}$	12	$(ClpP)_{14}$	1.2
	21[c]	$(ClpA)_6$·$(ClpP)_{14}$	1.5
	27[c]	$(ClpA)_6$·$(ClpP)_{14}$·$(ClpA)_6$	1.8

[a] Using the Beckman model E analytical ultracentrifuge with schlieren optics (see Figure 1). The buffer used was 50 mM Tris-HCl, pH 7.5, 1 mM EDTA, 0.3 M KCl, 1 mM DTT, 2 mM ATPγS, 25 mM $MgCl_2$, and 10% (v/v) glycerol. [b] The frictional ratio f/f_0 has been calculated from the frictional coefficient [$f = [M(1 - \bar{v}\rho)]/Ns$) and from the frictional coefficient of a sphere having a volume equal to that of the ellipsoid: $f_0 = 6\pi\eta(3M\bar{v})/4\pi N)^{1/3}$. [c] In two separate experiments with either ClpA hexamer in 2-fold or ClpP tetradecamer in 5-fold molar excess over the other component the variance for $s_{20,w}$ was ±1 S.

arated from each other and migrated as independent species with sedimentation coefficients similar to those measured when the proteins were alone (data not shown). In the presence of nucleotide, when ClpP was in excess the two fastest moving species had sedimentation coefficients of 21 and 27 S (Table 2), while the slowest sedimenting protein had a $s_{20,w}$ of 12 S, similar to that of ClpP alone (Table 1). Frictional coefficients (f/f_0) calculated for the smaller and the larger of the two complexes were 1.5 and 1.8, respectively. The estimated sizes of the complexes and the presence of free ClpP but not free ClpA suggest that the smaller associated species represents a 1:1 complex of ClpA hexamer and ClpP tetradecamer (calculated M_r 807 000) and the larger associated species represents a complex of 2 ClpA hexamers and 1 ClpP tetradecamer (calculated M_r 1 310 000). The existence of both of these species has been confirmed by electron microscopy (*24*). When ClpA hexamer was in excess of the ClpP tetradecamer, only free ClpA and the 2:1 complex were observed (Table 2). The high frictional coefficients, however, suggest that there is a sizable effect of molecular shape or volume on the hydrodynamic behavior of these complexes. It is interesting to note that the individual ClpP and ClpA oligomers also have larger frictional ratios than expected for compact globular proteins.

When ClpA and ClpP were mixed in a molar ratio of 2 $ClpA_6$:1 $ClpP_{14}$, quantitative ClpAP complexes were obtained after gel filtration in the presence of ATPγS (data not shown), which promotes more complete complex formation than previously seen with AMPPNP (*28*). In the presence of ATP, yields of ClpAP were very poor, because ClpA is degraded by ClpP (data not shown). ADP did not promote formation of the ClpAP complex and inhibited complex formation promoted by ATP (data not shown).

Stoichiometry of ClpA and ClpP in the Active Complex. The specific activities of ClpA and ClpP were determined in casein degradation assays in which either ClpP or ClpA was limiting in the presence of an excess of the other component and are listed in Table 3 for ClpA and ClpP. These specific activities have been obtained for many preparations of enzyme prepared over several years. Specific activities were 17 units/nmol of ClpP tetradecamer and 15 units/nmol of ClpA hexamer, indicating that a hexamer of ClpA can activate the casein degradation activity of a tetradecamer of ClpP. Because the complex has nearly

Table 3: Specific Activity of ClpA and ClpP[a]

	specific activity (mg of casein/h)	
	ClpA	ClpP
per milligram of protein	30 ± 5	55 ± 5
per nanomole of subunit	2.5	1.2
per nanomole of $ClpA_6$ or $ClpP_{14}$	15	16.8

[a] Clp protease activity was measured by the production of acid-soluble peptides from [^{3}H]-α-casein under standard conditions with saturating casein (see Experimental Procedures). Limiting ClpA or ClpP (0.1−0.2 μg) was added in the presence of an excess (10−20 μg) of the other component.

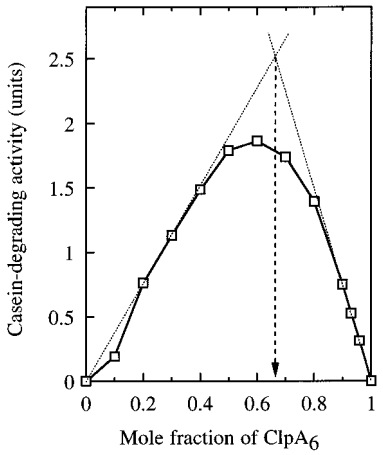

FIGURE 6: Stoichiometry of ClpA and ClpP in the active complex. The method of continuous variation was used with a total of 4 nM ClpA hexamer and ClpP tetradecamer. Casein degradation assays were conducted at 37 °C in the presence of excess (4 mM) ATP. Results are shown for a single set of assays with 4 nM total ClpA plus ClpP.

maximum activity when one ClpA hexamer is bound to one ClpP tetradecamer, the second hexamer of ClpA found in the 2:1 complex contributes little additional activating effect.

The ratio of ClpA to ClpP in the active complex was also determined by the method of continuous variation, in which casein degradation was measured with different molar ratios of ClpA hexamers and ClpP tetradecamers while maintaining a constant total molar concentration of the two (Figure 6). Highest activity was observed at a molar ratio of two hexamers of ClpA to one tetradecamer of ClpP. The identical result was obtained in a separate experiment with half the total concentration of the two proteins. A 2:1 ratio of $ClpA_6$ to $ClpP_{14}$ was optimal also for propeptide degradation in the presence of ATPγS, which requires formation of the ClpAP complex but no ATP hydrolysis (data not shown). The physical studies shown above indicate that when excess ClpA is present, the complex has two hexamers of ClpA and one tetradecamer of ClpP, and the Job analysis indicates that this 2:1 complex of ClpA and ClpP is active. Since the specific activities of ClpP calculated for the A_6:P_{14} and the $2A_6$:P_{14} complexes are the same, the second ClpA hexamer does not appear to activate ClpP for casein degradation.

Association Constant for ClpA and ClpP under Assay Conditions. Analysis of titration curves obtained by measuring proteolytic activity at varying ClpA or ClpP concentration in the presence of fixed amounts of the other component are shown in Figure 7. As either component was increased, activity showed a typical saturation function, indicative of

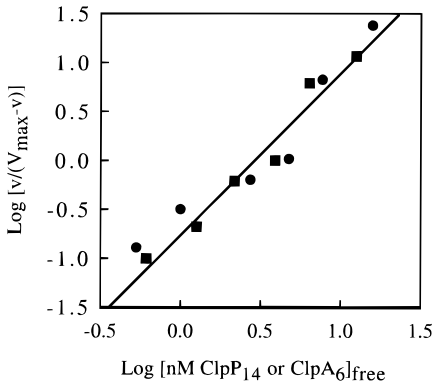

FIGURE 7: Concentration dependence for ClpA and ClpP for casein degradation. Casein degradation by ClpAP was assayed at 37 °C in standard assay mixtures with 4 mM ATP. Two sets of assays were performed with one component held constant and the other varied. Free concentrations of ClpA and ClpP were calculated assuming a 1:1 stoichiometry of the oligomers in the active complex (see text) and a direct proportionality between activity and complex formation.

the formation of a proteolytically active complex. Activity was proportional to the concentration of the limiting component, when the other component was present in excess. Bound ClpA or ClpP was calculated from the activity measured and the known specific activities, assuming that each bound oligomer had full activity, and the concentrations of the free components were then obtained by subtracting the amount bound from the total added at each point. From the midpoint of the saturation curves, estimated dissociation constants (K_d) of 25 ± 10 nM for ClpA subunit (4.2 nM hexamer) and 50 ± 15 nM for ClpP subunit (3.6 nM tetradecamer) in the complex were estimated.

DISCUSSION

ATP-dependent proteases are high molecular weight proteins found in the cytoplasm of bacterial cells or the cytosol and soluble compartments of organelles in eukaryotic cells. One exception is the membrane-bound *E. coli* FtsH protease (*7*) and its homologues found in mitochondrial membranes, which have membrane-spanning regions as well as a large soluble domain with ATPase and peptidase activity. All the proteases, including FtsH, are multimeric proteins, composed of multidomain polypeptides or complexes of separately encoded polypeptides with distinct ATPase, peptidase, and possibly other functions. The proteases whose structures have been determined by electron microscopy, the proteasome, ClpAP, ClpXP, and ClpYQ (HslUV), have very similar architectures. The proteases subunits form rings that stack together to make the proteolytic core, and an ATPase/chaperone or regulatory component binds on the outside face of each ring. In the case of ClpA, ClpX, and ClpY (HslU), the ATPase also forms a ring, giving the overall complex a barrel-like appearance. For the 26S proteasome, the ATPases might occupy similar positions as in Clp proteases, but additional factors are associated with the ATPases, giving the complex its unique saddlelike projection. The similarities in architecture among these divergent proteases suggests that the structure itself is integral to the proper biological and biochemical activities that they perform.

This paper has shown that ClpA and ClpP form a very tight complex in the presence of ATP, that the complex has

Scheme 1

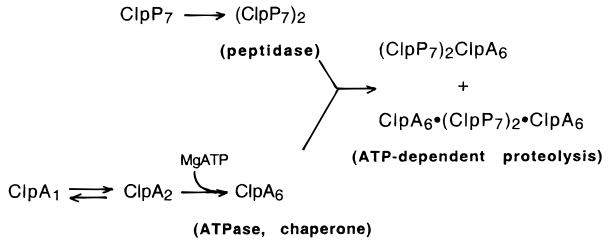

a defined stoichiometry of the oligomeric forms of ClpA and ClpP, and that the requirements for complex formation correlate with those for expression of enzymatic activity. Each homooligomer, as well as the 1:1 and 2:1 ClpAP complexes, behaves as discrete molecular species in solution, suggesting that interactions are very strong and the molecular species described are stable. Thus, the active form of ClpAP protease appears to be the complex of the oligomeric forms of ClpA and ClpP. In a separate study, we have obtained evidence that exchange of components from the various oligomers is very slow on the time scale of ATP hydrolysis and protein degradation and that these oligomers remain assembled during multiple catalytic cycles (S. K. Singh and M. R. Maurizi, unpublished results). The assembly and disassembly pathways found in vitro and the activities of the individual species are shown in Scheme 1.

The proteolytic active sites of Clp protease reside on ClpP, an oligomer of identical subunits arranged in two superimposed rings. ClpP alone has no proteolytic activity against high molecular weight substrates but can rapidly degrade proteins in the presence of ClpA and ATP (*12*, *18*, *20*, *21*, *32*). ClpA has been shown to have an ATP-dependent chaperonelike activity (*18*), and this activity may be required to partially unfold protein substrates to make them more susceptible to proteolysis by ClpP. Crystallographic analysis of ClpP has shown that ClpP resembles the 20S proteasome to the extent that the active sites are located in an aqueous cavity formed by the junction of the two proteolytic rings. Entry to the proteolytic core appears to be restricted to rather small axial channels (<15 Å in diameter). Protein substrates would need to be in an extended conformation to pass through the channels and reach the active sites. The structure of ClpAP suggests that access to the openings of the axial channels in ClpP is further limited by the binding of the ClpA to each face of ClpP, requiring that protein substrates interact with ClpA before being transferred to ClpP. Another function of ATP hydrolysis by ClpA would be to promote translocation of the unfolded substrate.

ATPase activity is not required for formation of ClpA hexamers. Therefore, binding of either ATP or specific nonhydrolyzable analogues of ATP must promote conformational changes in ClpA required for self-association. These conformational changes and others that occur upon hexamer formation in turn produce a form of ClpA that can interact strongly with ClpP. In contrast, ATP hydrolysis was required for assembly of the 26S proteasome (*40*). It is not clear whether assembly of the 26S proteasome has an energy requirement that is absent for assembly of ClpAP or whether this difference reflects unique conformational responses to binding of nucleotide analogues. ClpA, for example, requires 20-fold higher concentrations of AMPPNP than ATPγS for hexamer formation (data not shown).

One unusual finding in these studies was the high frictional ratios calculated for ClpA and ClpP as well as for the 1:1 and 2:1 $ClpA_6$:$ClpP_{14}$ complexes (Table 2). The axial ratios for ideal prolate or oblate ellipsoids calculated from these frictional ratios (*41*) suggest highly asymmetric molecules and are 3−5 times higher than those estimated from electron micrographs of ClpA, ClpP, or the ClpAP complexes (*24*). These data indicate that some structural feature contributes an unusual frictional drag on these molecules. One possible source of the discrepancy is the poorly defined mass adjacent to one ring of ClpA seen in electron micrographs and also visible in micrographs of the ClpAP complex. This mass could represent an unstructured portion of ClpA that extends out from the plane of the rings, giving the molecule an asymmetric shape. A second factor might be the presence of aqueous cavities or channels that increase the molecular volume. An aqueous cavity has been observed in ClpP (*24*, *39*) and a similar cavity in ClpA would seem to be necessary for binding and translocation of protein substrates (*3*). Such cavities would increase molecular volume and thereby reduce sedimentation rates.

When excess ClpA is present, the ClpAP complex has two hexamers of ClpA and one tetradecamer of ClpP. The Job analysis (Figure 6) indicates that optimal activity of ClpAP occurs with a 2:1 ratio of $ClpA_6$ to $ClpP_{14}$. However, since the specific activities of ClpP calculated for the A_6:P_{14} and the $2A_6$:P_{14} complex are nearly the same, the second ClpA hexamer does not appear to activate ClpP proportionately for casein degradation. This result is unexpected, because the high turnover number for oligopeptide degradation (*32*) suggests that peptide bond cleavage is not the rate-limiting step in degradation by ClpAP. One possibility is that substrates bound to ClpA on one side of the complex produce an inhibitory allosteric effect on the second ClpA, so that substrates are translocated only from one side at a time. Another possibility is that peptide products exit from the distal side of ClpP, inhibiting substrate binding or translocation by ClpA on that side. Experiments to address this issue further are underway.

Because inter-ring contacts appear weaker than intra-ring contacts, it is probable that assembly of ClpP proceeds by formation of heptameric rings followed by association of the rings. In this way, the assembly path for ClpP would be similar to that for the *Archaea* and *Rhodococcus* proteasomes, whose assembly has been studied in detail (*42*, *43*). The finding that ClpP rings could be reversibly dissociated was initially unexpected but is consistent with recent crystallograhic data (*39*). In ClpP, 34% of the surface area is buried in making intra-ring subunit contacts, which are stabilized by hydrophobic interactions, whereas only 8.5% of the surface area is buried in making contacts between the rings, which are stabilized mainly by hydrogen bonding (*39*).

The ease with which the rings can be dissociated in vitro raises the question of whether such dissociation or partial dissociation occurs also in vivo. Since the opposite face of the helix involved in interring contacts is part of the peptide binding pocket in the active site, such single rings of ClpP could have considerably altered substrate specificity or, more likely, impaired catalytic ability. Expression of activity by single rings of ClpP is being investigated. Perhaps more intriguing is the possibility that ionic changes in the active site cavity upon peptide bond cleavage might affect the interring contacts, leading to partial dissociation or other conformation changes that would produce ports through which peptides could escape. This effect would provide a means for peptide products to be released from the enzyme, a step for which no mechanism has at present been demonstrated or previously proposed.

REFERENCES

1. Goldberg, A. L. (1992) *Eur. J. Biochem. 203*, 9−23.
2. Gottesman, S., and Maurizi, M. R. (1992) *Microbiol. Rev. 56*, 592−621.
3. Maurizi, M. R. (1992) *Experientia 48*, 178−201.
4. Wojtkowiak, D., Georgopoulos, C., and Zylicz, M. (1993) *J. Biol. Chem. 268*, 22609−22617.
5. Rohrwild, M., Coux, O., Huang, H. C., Moerschell, R. P., Yoo, S. J., Seol, J. H., Chung, C. H., and Goldberg, A. L. (1996) *Proc. Natl. Acad. Sci. U.S.A. 93*, 5808−5813.
6. Kessel, M., Wu, W.-F., Gottesman, S., Kocsis, E., Steven, A., and Maurizi, M. R. (1996) *FEBS Lett. 398*, 274−278.
7. Tomoyasu, T., Gamer, J., Bukau, B., Kanemori, M., Mori, H., Rutman, A. J., Oppenheim, A. B., Yura, T., Yamanaka, K., Niki, H., et al. (1995) *EMBO J. 14*, 2551−2560.
8. Mizusawa, S., and Gottesman, S. (1983) *Proc. Natl. Acad. Sci. U.S.A. 80*, 358−362.
9. Torres-Cabassa, A. S., and Gottesman, S. (1987) *J. Bacteriol. 169*, 981−989.
10. Gottesman, S., Gottesman, M. E., Shaw, J. E., and Pearson, M. L. (1981) *Cell 24*, 225−233.
11. Aizenman, E., Engelberg-Kulka, H., and Glaser, G. (1996) *Proc. Natl. Acad. Sci. U.S.A. 93*, 6059−6063.
12. Katayama, Y., Gottesman, S., Pumphrey, J., Rudikoff, S., Clark, W. P., and Maurizi, M. R. (1988) *J. Biol. Chem. 263*, 15226−15236.
13. Gottesman, S., Clark, W. P., Crecy-Lagard, V. d., and Maurizi, M. R. (1993) *J. Biol. Chem. 268*, 22618−22626.
14. Lehnherr, H., and Yarmolinsky, M. B. (1995) *Proc. Natl. Acad. Sci. U.S.A. 92*, 3274−3277.
15. Schweder, T., Lee, K. H., Lomovskaya, O., and Matin, A. (1996) *J. Bacteriol. 178*, 470−476.
16. Laachouch, J. E., Desmet, L., Geuskens, V., Grimaud, R., and Toussaint, A. (1996) *EMBO J. 15*, 437−444.
17. Herman, C., Thevenet, D., D'Ari, R., and Bouloc, P. (1995) *Proc. Natl. Acad. Sci. U.S.A. 92*, 3516−3520.
18. Wickner, S., Gottesman, S., Skowyra, D., Hoskins, J., McKenney, K., and Maurizi, M. R. (1994) *Proc. Natl. Acad. Sci. U.S.A. 91*, 12218−12222.
19. Levchenko, I., Luo, L., and Baker, T. A. (1995) *Genes Dev. 9*, 2399−2408.
20. Hwang, B. J., Woo, K. M., Goldberg, A. L., and Chung, C. H. (1988) *J. Biol. Chem. 263*, 8727−8734.
21. Katayama-Fujimura, Y., Gottesman, S., and Maurizi, M. R. (1987) *J. Biol. Chem. 262*, 4477−4485.
22. Gottesman, S., Clark, W. P., and Maurizi, M. R. (1990) *J. Biol. Chem. 265*, 7886−7893.
23. Grimaud, R., Kessel, M, Beuron, F., Steven, A. C., and Maurizi, M. R. (1998) *J. Biol. Chem.* (in press).
24. Kessel, M., Maurizi, M. R., Kim, B., Trus, B. L., Kocsis, E., Singh, S. K., and Steven, A. C. (1995) *J. Mol. Biol. 250*, 587−594.
25. Hershko, A., and Ciechanover, A. (1992) *Annu. Rev. Biochem. 61*, 761−807.
26. Rechsteiner, M., Hoffman, L., and Dubiel, W. (1993) *J. Biol. Chem. 268*, 6065−6068.
27. Gottesman, S., Wickner, S., and Maurizi, M. R. (1997) *Genes Dev. 11*, 815−823.
28. Maurizi, M. R. (1991) *Biochem. Soc. Trans. 19*, 719−723.
29. Maurizi, M. R., and Ginsburg, A. (1995) *Biophys. J. 68*, A404.
30. Maurizi, M. R., Thompson, M. W., Singh, S. K., and Kim, S. H. (1994) *Methods Enzymol. 244*, 314−331.
31. Singh, S. K., and Maurizi, M. R. (1994) *J. Biol. Chem. 269*, 29537−29545.

32. Thompson, M. W., and Maurizi, M. R. (1994) *J. Biol. Chem. 269*, 18201−18208.
33. Maurizi, M. R., Clark, W. P., Katayama, Y., Rudikoff, S., Pumphrey, J., Bowers, B., and Gottesman, S. (1990) *J. Biol. Chem. 265*, 12536−45.
34. Shapiro, B. M., and Ginsburg, A. (1968) *Biochemistry 7*, 2153−2167.
35. Shrake, A., Whitley, E. J., Jr., and Ginsburg, A. (1980) *J. Biol. Chem. 255*, 581−589.
36. Zamyatnin, A. A. (1984) *Annu. Rev. Biophys. Bioeng. 13*, 145−165.
37. Muramatsu, N., and Minton, A. P. (1988) *Anal. Biochem. 168*, 345−351.
38. Flanagan, J. M., Wall, J. S., Capel, M. S., Schneider, D. K., and Shanklin, J. (1995) *Biochemistry 34*, 10910−10917.
39. Wang, J., Hartling, J. A., and Flanagan, J. (1997) *Cell 91*, 447−456.
40. Eytan, E., Ganoth, D., Armon, T., and Hershko, A. (1989) *Proc. Natl. Acad. Sci. U.S.A. 86*, 7751−7755.
41. Schachman, H. K. (1959) *Ultracentrifugation in Biochemistry*, Academic Press, New York.
42. Zwickl, P., Pfeifer, G., Lottspeich, F., Kopp, F., Dahlmann, B., and Baumeister, W. (1990) *J. Struct. Biol. 103*, 197−203.
43. Tamura, T., Nagy, I., Lupas, A., Lottspeich, F., Cejka, Z., Schoofs, G., Tanaka, K., Mot, R. D., and Baumeister, W. (1995) *Curr. Biol. 5*, 766−774.
44. Stafford, W. F., III (1992) *Anal. Biochem. 203*, 295−301.
45. Stafford, W. F., III (1996) *Biophys. J. 70*, A231.

BI973093E